ptx1, a Nonphototactic Mutant of *Chlamydomonas*, Lacks Control of Flagellar Dominance

Cynthia J. Horst and George B. Witman

Cell Biology Group, Worcester Foundation for Experimental Biology, Shrewsbury, Massachusetts 01545

Abstract. A new mutant strain of *Chlamydomonas*, *ptx1*, has been identified which is defective in phototaxis. This strain swims with a rate and straightness of path comparable with that of wild-type cells, and retains the photoshock response. Thus, the mutation does not cause any gross defects in swimming ability or photoreception, and appears to be specific for phototaxis. Calcium is required for phototaxis in wild-type cells, and causes a concentration-dependent shift in flagellar dominance in reactivated, demembranated cell models. *ptx1*-reactivated models are defective in this calcium-dependent shift in flagellar dominance. This indicates that the mutation affects one or more components of the calcium-dependent axonemal regulatory system, and that this system mediates phototaxis. The reduction or absence of two 75-kD axonemal proteins correlates with the nonphototactic phenotype. Axonemal fractionation studies, and analysis of axonemes from mutant strains with known structural defects, failed to reveal the structural localization of the 75-kD proteins within the axoneme. The proteins are not components of the outer dynein arms, two of the three types of inner dynein arms, the radial spokes, or the central pair complex. Because changes in flagellar motility ultimately require the regulation of dynein activity, cell models from mutant strains defective in specific dynein arms were reactivated at various calcium concentrations. Mutants lacking the outer arms, or the I1 or I2 inner dynein arms, retain the wild-type calcium-dependent shift in flagellar dominance. Therefore, none of these arms are the sole mediators of phototaxis.

THE unicellular biflagellate alga *Chlamydomonas* has been used extensively in the study of flagellar motility. This is due, in part, to the ease with which mutant strains displaying aberrant motility can be produced and analyzed. As a result, the structures which generate motility are well characterized, yet the processes which regulate motility remain obscure. To study the regulation of flagellar motility, we have generated mutant strains of *Chlamydomonas* which are defective in their ability to phototax.

The two flagella of *Chlamydomonas* can be distinguished based on their position relative to a specialized region of the chloroplast referred to as the eyespot (13). During phototaxis, the beat pattern of the *cis*-flagellum (the flagellum closest to the eyespot) and the *trans*-flagellum are modified, resulting in a change in swimming direction relative to the light. This requires that the *cis*- and *trans*-flagella respond differentially to the signal generated by photoreception. Previous studies have provided evidence that calcium is required for phototaxis (3, 4, 22, 25, 37). Moreover, the two flagella are differentially responsive to calcium, such that the *cis*-flagellum is more effective at force generation at low calcium (10^{-9} M), and the *trans*-flagellum more effective at higher calcium (10^{-7} M) (17). This differential sensitivity of the *cis*- and *trans*-flagella to calcium has been proposed to mediate the turning behaviors necessary for phototaxis (17).

We have identified a mutant strain of *Chlamydomonas*, *ptx1*, which specifically lacks the ability to phototax. This strain retains another light response, the photophobic or photoshock response, in which the cell responds to an abrupt increase in light intensity by transiently swimming backwards. Therefore, the phototactic and photoshock responses are genetically separable, and *ptx1* is competent for phototransduction. Experiments using reactivated cell models reveal that *ptx1* is specifically defective in the calcium-dependent shift in flagellar dominance seen in wild-type cells. This provides direct evidence that the differential sensitivity of the *cis*- and *trans*-flagella to calcium mediates phototaxis. The reduction or absence of a pair of 75-kD proteins correlates with the phototactic defect. Experiments to determine the structural location of the 75-kD proteins within the axoneme have excluded the outer dynein arm and two of the three types of inner dynein arms, the radial spokes, and the central pair complex. The precise location of these proteins remains obscure.

Materials and Methods

Cell Culture

Chlamydomonas reinhardtii wild-type strain 137^+ and all mutant strains were maintained in liquid culture as previously described (41). Cultures in log phase growth were used exclusively.

Mutagenesis

Wild-type cells were mutagenized using UV light following standard procedures (9). Irradiated cultures were enriched for cells which did not swim toward a stimulus light, the cells plated, and individual colonies tested for the ability to phototax. Cells of *ptx1*, one of several strains which appeared to be nonphototactic, were back-crossed to wild-type cells twice using standard procedures (9). The nonphototactic phenotype always segregated 2:2, indicating that the mutation affects a single locus.

Phototaxis of Individual Cells

The swimming behavior of individual cells was determined using a system originally developed by Morel-Laurens and Feinleib (23) and modified by A. G. Moss and G. B. Witman (manuscript in preparation). Briefly, a small chamber was designed that mounts directly on the microscope stage. Fiber optic cables were attached to opposite sides of the chamber to allow an argon ion laser stimulus light (488 nm) to be introduced from either direction. Swimming behavior was monitored with red light and recorded using a CCD video camera mounted on the microscope. Data collection began 30 s after light stimulation, and was continued for 2 min except for light-stimulated wild-type cells. In this case, phototaxis was so strong that by the end of the first minute of recording, all cells already had moved to the side of the chamber away from the light stimulus, and no additional cells passed through the region being recorded. Therefore, data from wild-type cells represents only the first minute of the data collection period. The *x,y* coordinates of each cell path were determined at 0.1-s intervals from the taped records using Expert Vision, a computer-assisted motion analysis system (Motion Analysis Corporation, Santa Rosa, CA). Circular statistics were used to calculate the mean vector of swimming for each cell (1). This calculation also generates an *r* value which provides a measure of the dispersion around the mean vector. The values for *r* range from 0 to 1, with 1 indicating a straight path. The mean vectors were grouped into 15° bins, and plotted on a polar histogram as the percentage of total cells falling within each bin. Thus, the direction of each line on the histogram represents the mean direction of the swimming path, and the length of each line represents the percentage of cell paths falling within that bin.

The Photophobic Response and Swimming Rate

The photophobic response and swimming rate were both quantitated using video microscopy. Cells were placed in a small plastic chamber and swimming paths of individual cells recorded using a CCD camera mounted on the microscope. To determine the percentage of cells which undergo the photophobic response, cells were first recorded under red light. Removal of the red filter provided an abrupt increase in light intensity to the cells sufficient to generate the photophobic response. Video recordings were analyzed to determine the percentage of cells in each field which responded to the increase in light intensity. To determine swimming rate, cells were video recorded (using red light to avoid phototactic and photokinetic effects) and tapes analyzed using Expert Vision (Motion Analysis Corporation, Santa Rosa, CA).

Determination of Eyespot Position

Cells were placed on silicon-coated slides and observed by dark field microscopy. The flagella rapidly stick to the silicon coating and glide in opposite directions, so that the cell body is observed axially with the two flagella stuck to the slide at a 180° angle. The position of the eyespot on the cell body is then assessable relative to the line of the flagella.

In Vitro Calcium Depletion

Cells were washed three times in HES (10 mM Hepes, pH 7.3, 0.5 mM EGTA, 4% sucrose) and observed by dark-field microscopy (17). Swimming behavior was monitored between 15 and 30 min after the first resuspension in HES.

Reactivated Cell Models

Cell models were produced and reactivated as previously described (10, 15, 17). Briefly, cells were washed two times by centrifugation at 1,100 *g* and resuspended in HES. Cells were demembranated by dilution of 10 μl concentrated cells into 100 μl ice-cold demembranation buffer (30 mM Hepes, pH 7.3, 5 mM $MgSO_4$, 1 mM DTT, 1 mM EGTA, 50 mM KAcetate, 1% polyethylene glycol [20 kD], 0.1% NP-40). Cell models were further diluted 1:10 into ice-cold reactivation buffer (30 mM Hepes, pH 7.3, 5 mM $MgSO_4$, 1 mM DTT, 50 mM KAcetate, 1% polyethylene glycol, 1 mM ATP, and $CaCl_2$ and EGTA adjusted to give either 10^{-9} M Ca^{+2}, or 10^{-7} M Ca^{+2} as described in Bessen et al. [2]). After a 5-min preincubation, cell models were observed for 10 min by dark-field light microscopy.

Isolation and Fractionation of Axonemes

Isolated axonemes were produced following the procedure of Witman (39). High salt extraction and sucrose density gradient centrifugation followed the procedure of King et al. (20), omitting dialysis of the high salt extract.

Two-Dimensional Gel Electrophoresis

Two-dimensional gel electrophoresis was performed by a modification of previously described procedures (7, 27, 31). Denaturation buffer (0.3 M Tris, pH 8.8, 5% SDS, 0.01% EDTA, 1% β-mercaptoethanol) was added to the pellet of isolated axonemes (final protein concentration of 20 mg/ml), and the sample heated at ~100°C for 4 min. 10 μl of NP-40 was then added to 10 μl of sample (200 μg total protein) and gently mixed, followed by the addition of 60 μl of sample buffer (9.5 M urea, 8% NP-40, 5% β-mercaptoethanol, 2% pH 3.5–10 ampholine). The NEPHGE dimension was run as a slab gel composed of 8.6 M urea, 3.75% acrylamide, 1.9% NP-40, 6% ampholines (pH 3.5–10, 9–11, 4–6, and 5–7 mixed in a ratio of 1:0.22:0.07:0.07). The gel was polymerized for 2 h using fluorescent lights after the addition of 0.9 mM riboflavin, 0.0025% N,N,N',N'-tetramethylethylenediamine. Samples were overlayed with a solution containing 5 M urea, 2% pH 5–7 ampholine, 0.5% pH 3.5–10 ampholine, and run from the anode for 16 h at 2 mA constant current. The anode buffer was 10 mM H_3PO_4, the cathode buffer 20 mM NaOH. Lanes cut from the NEPHGE slab gel were covered with equilibration buffer (0.0625 M Tris, pH 6.8, 10% SDS) and transferred immediately to the stacking gel of the second dimension. The SDS-polyacrylamide gel for the second dimension was composed of 5–15% acrylamide and 0–2.4 M glycerol gradients as described by King et al. (19). Proteins were revealed by silver stain (24).

Electron Microscopy

Isolated axonemes were fixed at room temperature for 15 min in 1% glutaraldehyde in 30 mM Hepes, 5 mM $MgSO_4$, 1 mM DTT, 0.5 mM EDTA, 50 mM KAcetate, pH 7.4, then centrifuged at 27,000 *g* for 15 min. The resulting pellet was further fixed for 50 min in 1% glutaraldehyde, 50 mM cacodylate buffer, pH 7.4, washed with cacodylate buffer, postfixed for 1 h in 1% OsO_4, dehydrated and embedded. Thin sections were stained with uranyl acetate and lead citrate.

Results

ptx1 Specifically Lacks the Ability to Phototax

The ability of wild-type and *ptx1* cells to phototax in response to a directional light stimulus was assessed using video microscopy and computer-assisted motion analysis. The mean direction of travel (i.e., the mean vector of each cell path) was determined, and the results plotted as a polar coordinate histogram (Fig. 1). The angle of each line on the histogram represents the direction of the mean vector of swimming as grouped into 15° bins. The length of each line represents the percentage of the total number of cells whose mean vector of travel fell within that bin. The swimming paths of unstimulated cells from both wild-type and *ptx1* strains were evenly distributed (Fig. 1, *A* and *C*), indicating that path direction is random in unstimulated cells. After the onset of the light stimulus, wild-type cells swam almost directly away from the incoming light (Fig. 1 *B*); that is, they are negatively phototactic. In contrast, the *ptx1* cell paths remained distributed in all directions (Fig. 1 *D*), indicating that these cells lack the phototactic response.

Potentially, the failure to phototax could result from any major change that grossly affects the cell's ability to swim, such as changes in flagellar coordination or waveform.

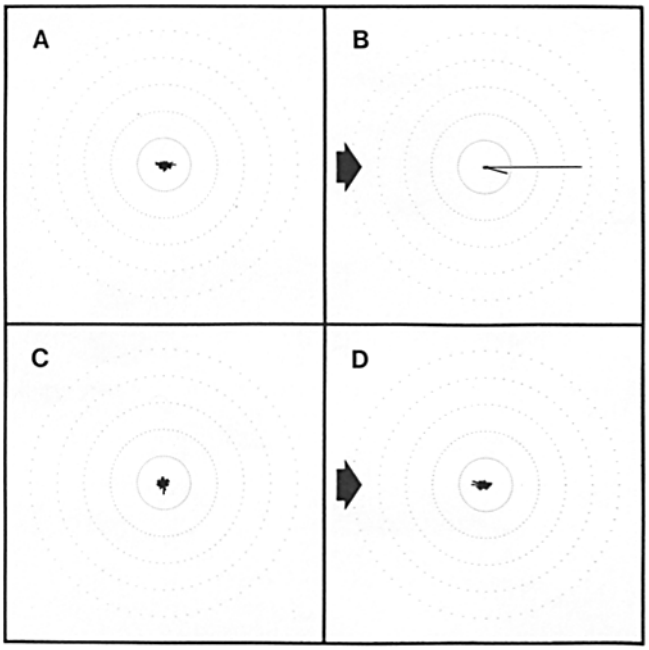

Figure 1. Polar histogram illustrating swimming direction of wild-type and *ptx1* cells. When present, the stimulus light was introduced from the left as indicated by the arrows. (*A*) Wild-type cells, unstimulated, $n = 370$; (*B*) wild-type cells, stimulated, $n = 199$; (*C*) *ptx1* cells, unstimulated, $n = 319$; and (*D*) *ptx1* cells, stimulated, $n = 359$. Each line represents the percentage of individual cell paths whose mean vector of travel falls within that 15° bin. Each annulus equals 20% of the total number of cells.

Swimming rates were assessed to determine if the *ptx1* defect is specific for phototaxis and not a general motility defect. The swimming rates of wild-type and *ptx1* cells were identical (Table I). Thus, the mutant flagella are capable of producing force comparable that of wild type, indicating that the basic machinery required to generate flagellar motility remains intact in the mutant strain. The failure to phototax might also result if cells have a tendency to frequently change directions or circle, such that their progress is severely impeded. A measure of the straightness of the swimming paths analyzed in Fig. 1 can be calculated, and is referred to as the r value. The values for r range from 0 to 1, with $r = 1$ indicating that the cell path was perfectly straight. The r values for wild-type and *ptx1* cells were indistinguishable in the light (Table I) and dark (not shown), reinforcing the conclusion that the mutation does not produce gross motility defects and is specific for phototaxis.

Phototransduction is thought to occur in the region of the eyespot. Because defects in phototaxis have previously been reported in mutant strains with abnormal eyespots (23), cells were observed by dark field microscopy to assess the presence and position of the eyespot. The eyespot was clearly evident in *ptx1* cells and was located approximately 45° from the plane of the flagella, as is seen in wild-type cells (32, data not shown).

Chlamydomonas displays two types of responses to light. In addition to the phototactic response, wild-type cells react to an abrupt increase in light intensity with a photophobic or photoshock response. In this response, the flagella are briefly thrown forward, and change from an asymmetric to a symmetric waveform, causing the cell to move transiently backward. Comparison of the percentage of cells which underwent the photophobic response after an abrupt increase in light intensity showed that wild-type and *ptx1* cells respond comparably (Table I). This indicates that *ptx1* cells are competent for photoreception, and suggests that the lack of phototaxis is not simply due to an inability to detect light. Additionally, this demonstrates that the photophobic response and phototaxis are genetically separable.

Table I. Comparison of Swimming Behaviors of Wild-type and ptx1 *Cells*

	Swimming rate		Path straightness		Photophobic response	
	μm/s	SD	r	SD	Percent responding	SD
Wild type	105.8	21.3	0.82	0.21	84.7	13.7
ptx1	104.2	18.4	0.84	0.20	92.6	6.0

The numbers of cells scored were 85, 199, and 133 for wild type, and 121, 359, and 191 for *ptx1*.

Responses to Calcium

The lack of phototaxis in *ptx1*, while the photophobic response is retained, suggests that the defect affects the behavioral repertoire of the flagella, rather than photoreception. A previous report demonstrated a differential sensitivity of the *cis*- and *trans*-flagella to calcium, and proposed that this difference mediates phototaxis (17). Wild-type cells suspended in Ca^{2+}-free medium tended to swim in circles with the *cis*-flagellum dominant, rather than in the normal straight or slightly helical paths observed in normal medium (17). This change in swimming behavior was presumably due to the depletion of intraflagellar calcium. As an initial test of the mutant's ability to respond to different calcium concentrations, wild-type and *ptx1* cells were observed after resuspension in buffer containing 0.5 mM EGTA, and categorized as (*a*) swimming in circles or in an erratic helix (one flagellum was held forward beating with a very shallow waveform, while the other flagellum beat apparently normally); (*b*) swimming straight; or (*c*) dead or damaged. As previously reported, wild-type cells tended to circle in the EGTA-containing buffer (Fig. 2) (17). In contrast, *ptx1* cells continued to swim with a smooth, straight path (Fig. 2). Assuming that intracellular Ca^{2+} was depleted in both *ptx1* and wild-type cells under these conditions, the lack of a response in *ptx1* indicates that its flagella do not respond normally to changes in calcium concentration.

As a more direct test of the ability of *ptx1* axonemes to respond differentially to calcium concentrations in the submicromolar range, the effect of calcium on axonemal dominance was determined by reactivation of detergent-extracted cell models at either 10^{-9} or 10^{-7} M Ca^{2+}. After reactiva-

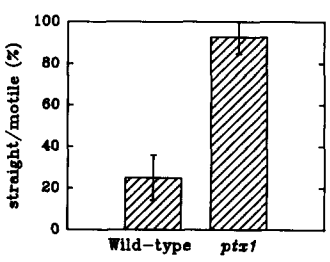

Figure 2. In vivo flagellar inactivation. Wild-type and *ptx1* cells were resuspended in buffer containing 0.5 mM EGTA and scored for whether one flagellum became dominant vs straight swimming. Each bar represents six trials. The total number of cells was 214 for wild type and 173 for *ptx1*.

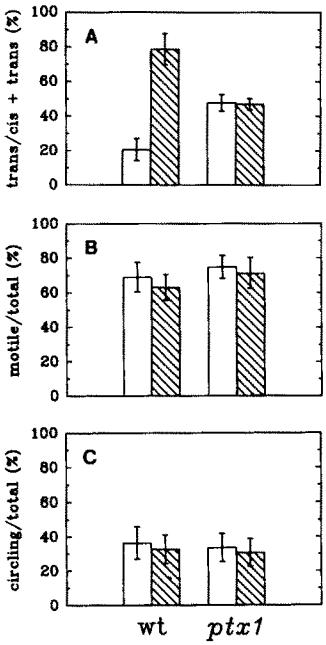

Figure 3. Calcium-dependent flagellar dominance in reactivated cell models. (*A*) The percentage of cell models that were *trans*-dominant among circling cells in which the *cis*- and *trans*-flagella could be identified; (*B*) the percentage of total cells which were motile; and (*C*) the percentage of total cells which were circling. (□) Cell models reactivated at 10^{-9} M Ca^{2+}; (▨) cell models reactivated at 10^{-7} M Ca^{2+}. Each bar represents at least sixteen trials, with a minimum of 1,610 cells in *A*, and 4,638 cells in *B* and *C*.

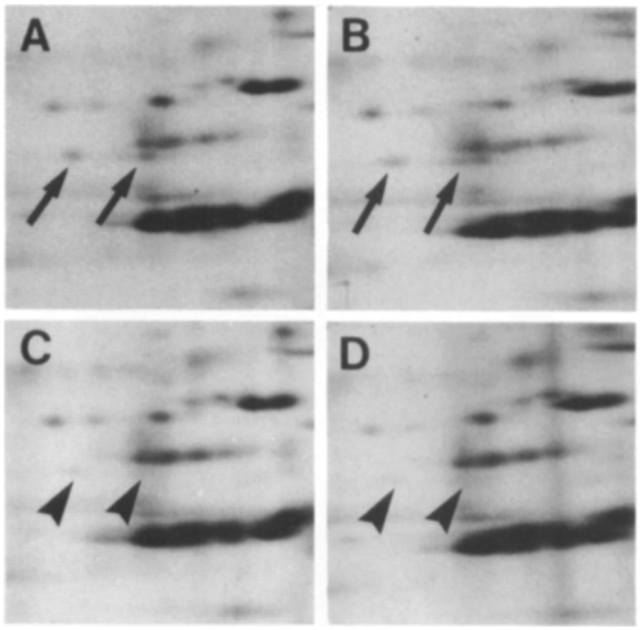

Figure 5. 75-kD region of two-dimensional gels of axonemes isolated from the tetrad products of a single zygote. (*A* and *B*) Phototactic; (*C* and *D*) nonphototactic. The arrows and arrowheads indicate the migration position of the 75-kD proteins when the proteins are present, and reduced or absent, respectively.

tion, cell models were observed and placed into one of five categories: (*a*) circling, *cis*-flagellum dominant; (*b*) circling, *trans*-flagellum dominant; (*c*) circling but the eyespot was not evident, so that the *cis*- and *trans*-flagella could not be identified; (*d*) swimming straight or helically; or (*e*) nonreactivated or damaged. As previously reported (17), wild-type cell models reactivated at 10^{-9} M Ca^{2+} tended to swim in circles with the eyespot directed outward. Thus, under these conditions, the *cis*-flagellum was dominant in determining the direction of circling, and the percentage that were *trans*-dominant was low (Fig. 3 *A*). Wild-type cell models reactivated at 10^{-7} M Ca^{2+} tended to circle with the eyespot directed toward the center of the circle. In this case the *trans*-flagellum was dominant in determining the direction of circling (Fig. 3 *A*). In contrast to wild-type cell models, *ptx1* cell models appeared to lack control over which flagellum became dominant. The percentage of total cell models that circled was the same as in wild type (Fig. 3 *C*),

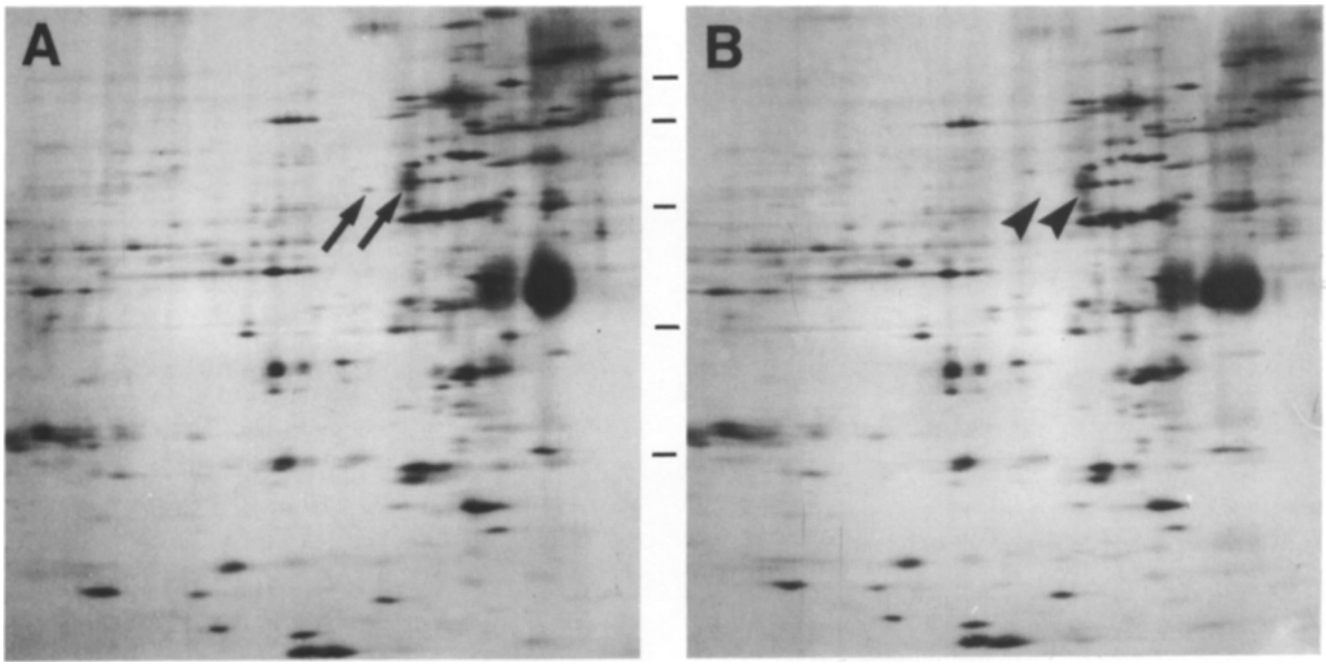

Figure 4. Silver-stained two-dimensional gels of isolated axonemes. (*A*) Wild-type cells, and (*B*) *ptx1* cells. Arrows indicate the positions of the 75-kD proteins in wild type, and arrowheads their expected positions in *ptx1*. The IEF dimension is oriented with acidic proteins to the right. Markers between the gels indicate the migration positions of 116-, 97-, 66-, 45-, and 31-kD molecular mass markers.

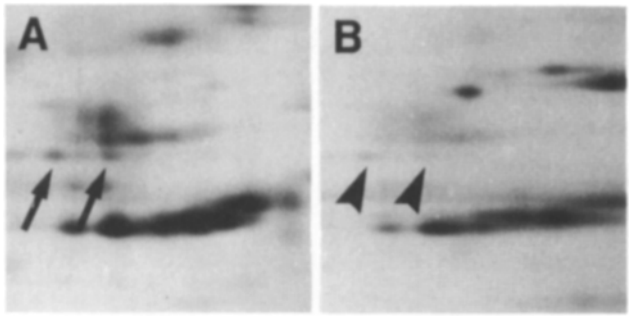

Figure 6. Silver-stained two-dimensional gels illustrating high-salt extractability of the 75-kD proteins. Supernatant (*A*) and pellet (*B*) fractions generated following 0.6 M NaCl extraction of wild-type axonemes. The pellet was resuspended to the same volume as the supernatant and equal volumes loaded on the gel. Only the region of the 75-kD proteins is shown. Arrows and arrowheads are as in Fig. 4.

but ~50% of the circling cell models were *trans*-flagellum dominant and 50% *cis*-flagellum dominant regardless of the calcium concentration (Fig. 3 *A*). The percentage of total wild-type and *ptx1* cell models that were motile was the same regardless of the calcium concentration (Fig. 3 *B*). Thus, although *ptx1* clearly is defective in the ability of its axonemes to respond differentially to calcium, this defect is manifested differently in demembranated cell models than in living cells (see Discussion). More importantly, the clear correlation between the inability to phototax and the inability to differentially regulate *cis*- and *trans*-flagellar motility in *ptx1* provides the most compelling evidence to date that the calcium-dependent shift in flagellar dominance mediates phototaxis.

Identification of Axonemal Components Correlated with the ptx1 *Defect*

The abnormal response of detergent-extracted, reactivated *ptx1* cell models to calcium suggests that the defect resides in the axoneme itself. To identify axonemal components affected by the *ptx1* mutation, isolated axonemes prepared from wild-type and *ptx1* cells were analyzed by gel electrophoresis. No differences in the dynein heavy chains were observed between mutant and wild-type axonemes after separation on 3–5% acrylamide, 2–8 M urea gels (19) to resolve the high molecular weight proteins (data not shown). Among the over 200 proteins resolved by two-dimensional gel electrophoresis, the only consistent differences observed between wild-type and *ptx1* were at 75 kD. Two spots were identified which were consistently missing or greatly diminished in the mutant axonemes (Fig. 4). The distribution of the 75-kD proteins was determined in five full tetrad sets from back-crosses between *ptx1* and wild-type cells. In all cases, the lack of phototaxis cosegregated with the absence or marked reduction of the 75-kD proteins (Fig. 5). Thus, the probability is at least 96.9% that the lack of the 75-kD polypeptides is related to the *ptx1* mutation. These proteins fractionate exclusively with the axoneme and are not found in the membrane/matrix fraction (data not shown).

Localization of the 75-kD Proteins Within the Axoneme

Because the 75-kD proteins are associated with phototaxis, their localization would reveal which axonemal structures participate in the regulation of flagellar beat pattern. Two approaches were used in attempting to localize the 75-kD proteins: fractionation of the axoneme, and analysis of mutant strains with known structural defects. The mutant strains were examined with regard to both the presence or absence of the 75-kD proteins, and retention of the calcium-dependent shift of flagellar dominance in reactivated cell models.

Isolated axonemes from wild-type cells were extracted with 0.6 M NaCl, and the salt-extractable components separated from the remainder of the axoneme by centrifugation. This procedure extracts most of the dynein arms and many uncharacterized proteins, while leaving the radial spokes associated with the axoneme (31). Comparison of two-dimensional gels of the high-salt supernatant versus the pellet revealed that the 75-kD proteins were extracted with high salt (Fig. 6), indicating that they are not stable components of the radial spokes. The salt-extractable components were

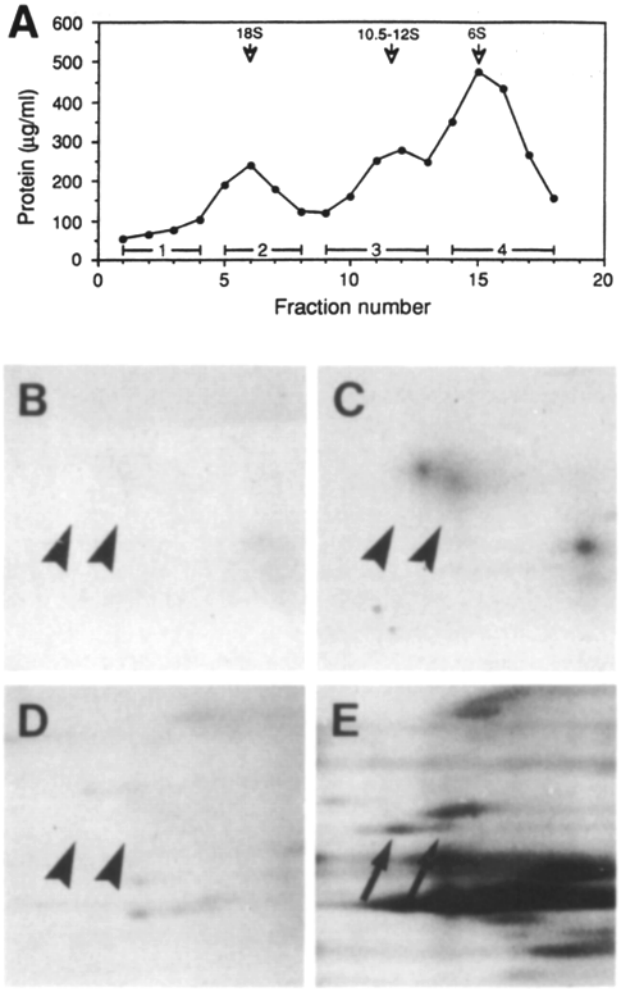

Figure 7. Distribution of the 75-kD proteins after sucrose density gradient centrifugation. (*A*) High-salt extractable components from wild-type axonemes were separated on a 5–20% continuous sucrose gradient, and fractions pooled as indicated by the bars. Approximate sedimentation values are given above each peak. Each pool was then analyzed by silver-stained two-dimensional gels to determine the distribution of the 75-kD proteins. (*B*) Pool 1; (*C*) pool 2; (*D*) pool 3; and (*E*) pool 4. Only the portion of the gel containing the 75-kD proteins is shown. Arrows and arrowheads are as in Fig. 4.

further fractionated by sucrose density gradient centrifugation. Fractions from the sucrose gradient were pooled based on peaks of protein distribution (Fig. 7 *A*). Previous studies have shown that the 10.5–12 S and 18 S fractions contain dyneins (29), whereas the 6 S fraction contains a complex mixture of proteins. Each pool was analyzed on two-dimensional gels to determine the distribution of the 75-kD proteins within the sucrose gradient. In agreement with previous work, pools 2 and 3 contained predominantly dynein proteins, and pool 1 contained only trace amounts of dynein (Fig. 7, *B–D*) (29). Both 75-kD proteins were found in pool 4, which includes the 6 S protein peak (Fig. 7 *E*). This distribution does not reveal the structural location of the 75-kD proteins, but does indicate that they are not stable components of the dynein arms.

The location of the 75-kD proteins was further investigated through the comparison of two-dimensional gels of axonemes isolated from mutant strains with known structural defects. Three strains, *oda1*, *ida1* and *ida4*, missing the outer arms, the I1 inner arms and the I2 inner arms, respectively (16, 18), retain the 75-kD proteins (Fig. 8, *C–E*). This is consistent with the results shown in Fig. 7 in which the 75-kD proteins did not segregate on the sucrose density gradient with the dynein arm subunits. Mutant strains *pf14* and *pf18*, lacking the radial spokes and central pair complex, respectively, also retain the 75-kD proteins (Fig. 8, *F* and *G*). The mutant lacking the central pair complex may show a slight reduction of the 75-kD proteins, possibly suggesting an association between the central pair complex and these proteins. However, the extent of the reduction is not comparable with that of the central pair complex proteins, nor to that observed in *ptx1*. Additionally, the 75-kD proteins are retained in the mutant strain *uni1* which lacks the *cis*-flagellum (Fig. 8 *H*). If the single flagellum present on *uni1* represents a true *trans*-flagellum, this result would indicate that the 75-kD proteins are not differently segregated between the two flagella. If they were uniquely segregated to the *trans*- or *cis*-flagellum, then they would be either significantly enhanced or absent, respectively, in *uni1*. Electron microscopic studies also failed to reveal any structural differences between axonemes of *ptx1* and wild type (data not shown). Thus, the 75-kD proteins are not components of any of the major axonemal structures, and their location remains unknown.

The Role of Specific Dynein Arms in the Differential Flagellar Response to Calcium

The role of dynein arms in the differential response of the *cis*- and *trans*-axonemes to calcium was investigated directly using reactivated cell models of the mutant strains missing specific sets of dynein arms described above. All three strains, *oda1*, *ida1*, and *ida4*, retain the calcium-dependent shift in flagellar dominance (Fig. 9). Thus, none of these subsets of dynein arms are exclusively responsible for mediating calcium effects on flagellar dominance.

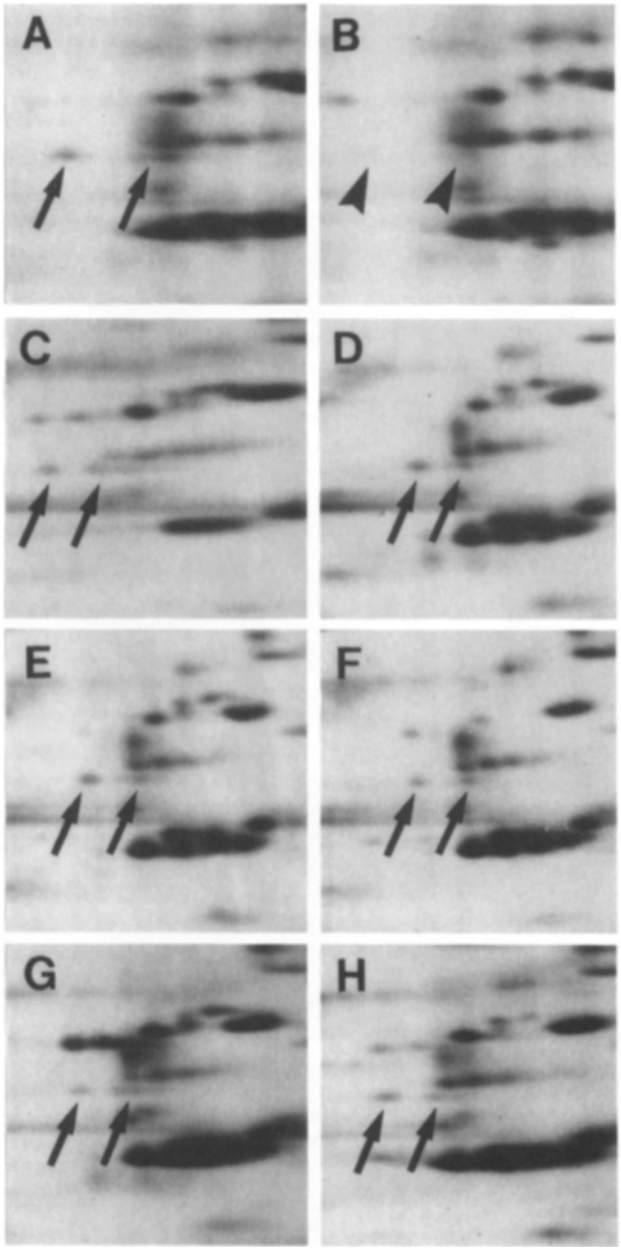

Figure 8. Silver-stained two-dimensional gels of isolated axonemes from mutant strains with known structural defects. (*A*) wild type; (*B*) *ptx1*; (*C*) *oda1*, missing the outer dynein arms; (*D*) *ida1*, missing the inner dynein arm I1; (*E*) *ida4*, missing the inner dynein arm I2; (*F*) *pf14*, missing the radial spokes; (*G*) *pf18*, missing the central pair complex; and (*H*) *uni1*, missing the *cis*-flagellum. Only the region of the 75-kD proteins is shown. Arrows and arrowheads are as in Fig. 4.

Discussion

Phototaxis in *Chlamydomonas* is a complex behavior initiated by the absorbance of light and resulting in an alteration of flagellar motility to produce changes in swimming direction. The action spectrum for phototaxis, as well as the effects of specific retinal analogues, suggests that a rhodopsin-like pigment serves as the chromophore (6, 11, 38). Rhodopsin is thought to be localized to the plasma membrane overlying the eyespot on the cell body (21). The eyespot itself is a specialized region of the chloroplast composed of stacks of carotenoid-containing lipid granules which may function as a quarter-wave stack (5). The cell rotates as it swims, and alternate reflection from, and shading by, the eyespot presumably causes a cyclic amplification and diminution of the light signal which provides directional information to orient the cell. Because calcium is required for phototaxis (4, 22, 25,

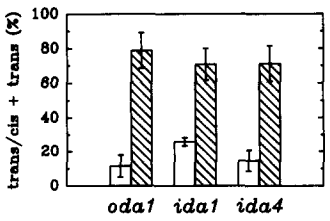

Figure 9. Calcium-dependent flagellar dominance in reactivated cell models from strains defective in dynein arms. (*A*) *oda1*; (*B*) *ida1*; and (*C*) *ida4*. (□) Cell models were reactivated at 10^{-9} M Ca^{2+}. (▨) Cell models were reactivated at 10^{-7} M Ca^{2+}. Each bar represents at least four trials, with a minimum of 300 total cells.

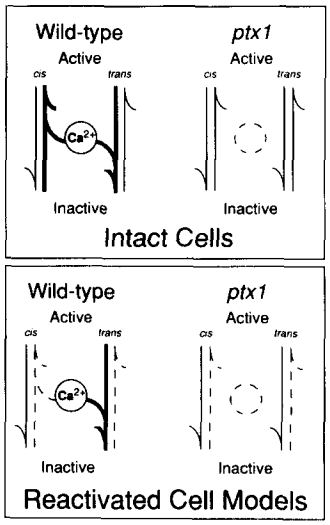

Figure 10. Model of calcium effects in intact cells vs. reactivated cell models. See discussion for explanation. Circles indicate a calcium-sensitive switch that shifts the equilibrium between activity and inactivity in the direction indicated. Responses at 10^{-9} M Ca^{2+} are illustrated. At 10^{-7} M Ca^{2+}, the calcium-sensitive switch would shift the equilibrium in the opposite direction. The calcium-sensitive switch is missing in *ptx1*.

26), light absorption is thought to result either directly or indirectly in a change in intracellular free calcium, which in turn alters flagellar motility.

Phototaxis, however, requires not only that the cell can regulate flagellar motility, but that it can differentially regulate its two flagella in order to turn. Consistent with the above model, the two axonemes have been shown to be differentially sensitive to calcium. When demembranated cell models are reactivated at 10^{-9} M Ca^{2+} the *cis*-axoneme is more efficient at force generation, whereas at 10^{-7} M Ca^{2+} the *trans*-axoneme is more efficient (17). This disparate responsiveness to calcium was proposed to mediate phototaxis. The mutant strain *ptx1* provides direct evidence for this model. Because this strain swims at a normal rate, the basic flagellar machinery necessary to produce force is not affected by the mutation, and the lack of phototaxis cannot be explained simply by gross changes in cell motility. *ptx1* is capable of phototransduction as evidenced by the retention of the photoshock response. Additionally, the defect is not due to mispositioning of the eyespot. The eyespot is located ~45° from the line of the flagella, where it presumably is associated with one of the microtubule rootlets, as in wild-type cells (12). Although the eyespot is correctly positioned relative to the plane of the flagella, the *cis*- and *trans*-flagella potentially could be reversed, such that the flagellum which biochemically represents the *trans*-flagellum is located closest to the eyespot. If this were the case, the flagellar responses would be inverted relative to the eyespot, causing a photostimulated cell to swim in an abnormal path as it continually tried, and failed, to orient to the light. However, *ptx1* cells continued to swim normally when photostimulated. The result that ~50% of reactivated cell models were *cis*-axoneme dominant and 50% *trans*-axoneme dominant at both 10^{-9} and 10^{-7} M Ca^{2+} might arise if the eyespot were randomly distributed on opposite microtubule rootlets. Yet, if this were the case, 50% of the cells would be phototactic, which was not observed. The most striking feature of *ptx1* is that it does not display the normal calcium-dependent shift in flagellar dominance. Thus, the calcium-dependent control of flagellar dominance is related to, and necessary for, phototaxis.

The observation that *ptx1* is defective in phototaxis, yet retains the ability to undergo the photoshock response, provides the first evidence that these two processes are genetically separable. This indicates that although the pathways leading to phototaxis and the photoshock response both use calcium, they differ in at least some components.

Potentially, flagellar dominance could be accomplished through changes in flagellar waveform, beat frequency, or both. The *cis*- and *trans*- flagella have been shown to have intrinsically different beat frequencies (15, 33), a difference which is retained in reactivated cell models (15). Because this difference was not seen when dynein arms extracted from wild-type axonemes were added back to cell models of outer arm deficient mutants, it was proposed that the difference may be due to posttranslational modifications differentially imparted onto the outer dynein arms of the *cis*- and *trans*-flagella (36). While this may be the case, current evidence argues against changes in beat frequency mediating phototaxis. When beat frequencies of the *cis*- and *trans*-axonemes of cell models were measured after reactivation at 10^{-9} or 10^{-7} Ca^{2+}, no shift was observed and the beat frequency of the *trans*-axoneme was higher at both calcium concentrations (15). Additionally, studies using single cells captured on a micropipette revealed that, although changes in beat frequency were observed after light stimulation, the *cis*- and *trans*-flagella changed beat frequency concurrently (34). An extension of these studies revealed opposing changes in flagellar waveform of the *cis*- and *trans*-flagella after light stimulation (35). This is consistent with the changes observed in the axonemal waveform of reactivated cell models used in the present study (data not shown) and with the progressive inactivation previously described (17). Thus, it is likely that changes in effective force generation are predominantly mediated by changes in flagellar waveform.

In wild-type cells, the disparate responses of the *cis*- and *trans*-axonemes to calcium requires differential sorting of specific axonemal components between the two flagella. This could occur at two levels. One possibility is that the *cis*- and *trans*-axonemes are imparted with different proteins which respond to calcium concentration; alternatively, the calcium-sensitive component of the regulatory system could be identical in the two axonemes, but other components which relay information from the calcium sensor to the effector, or the effectors themselves, could be different. *ptx1* cell models appear to have lost the ability of both the *cis*- and *trans*-flagella to respond to submicromolar levels of calcium. Therefore, *ptx1* probably is defective in a critical component of the calcium regulatory machinery that is common to both axonemes. This is consistent with our observation that the pair of 75-kD proteins reduced or absent in *ptx1* are neither missing nor enriched in flagella of *uni1*.

It is particularly intriguing that although living *ptx1* cells continued to swim straight under conditions designed to de-

plete intraflagellar calcium, the axonemes of *ptx1* demembranated cell models appeared to be randomly inactivated at both 10^{-9} and 10^{-7} M Ca^{2+}. The following model provides one possible explanation for this result (Fig. 10). In living, unstimulated wild-type cells, there is a balance within each flagellum between biochemical processes tending toward axonemal activation and inactivation. Upon photostimulation, changes in intraflagellar calcium concentration activate a calcium-sensitive switch that momentarily shifts the equilibrium in each flagellum toward activation or inactivation, causing transient alteration of the beat pattern. Opposing responses by the *cis*- and *trans*-flagella cause the cell to turn toward or away from the light. In *ptx1*, the calcium sensor is missing, so that changes in intraflagellar calcium have no effect on the balance of beating, and the cells continue to swim straight. Upon demembranation of wild-type cells, loss of a critical component causes the equilibrium in both axonemes to be shifted toward inactivation, but the calcium-sensitive switch accelerates the inactivation in an axoneme-specific manner, leading to the observed *cis*- or *trans*-axonemal dominance. In demembranated *ptx1* cells, the equilibrium is also shifted toward inactivation, but because there is no calcium-sensitive switch to selectively accelerate inactivation of one of the two axonemes, both axonemes are inactivated at about the same rate and it is simply a matter of chance whether the *cis*- or *trans*-axoneme is beating more effectively in a given cell. Other, more complex, models could be proposed to reconcile the differences in the observations on living and demembranated *ptx1* cells, but presently there is insufficient information to distinguish between the possible models. What is clear is that the system responsible for the differential control of *cis*- versus *trans*-flagellar activity is complicated, and that an understanding of the system will require more information on the biochemical processes that result in inactivation, and on the individual components involved in this regulation.

Two proteins have been identified which may be components of the regulatory system. The loss of phototaxis in *ptx1* correlates with the loss or reduction of a pair of previously undescribed 75-kD axonemal proteins. Fractionation of the axoneme revealed that both of these proteins are extracted by 0.6 M NaCl, suggesting they are not components of the radial spokes, which remain with the axoneme under these conditions (30). Additionally, the proteins sediment at ~6 S in sucrose density gradients, indicating that they are not stable components of any of the dynein arms (29).

The structural location of the 75-kD proteins within the axoneme was further investigated through analysis of two-dimensional gels of axonemes isolated from mutant strains with known structural defects. Strains missing the outer dynein arm (*oda1*), or inner dynein arms I1 or I2 (*ida1* and *ida4*, respectively) retained the 75-kD proteins. This is consistent with reactivated cell model studies wherein each of these strains retained the calcium-mediated shift in flagellar dominance seen in wild-type cells. Because dynein is the force-generating molecule which produces flagellar motility, regulation of phototaxis ultimately must be accomplished through the regulation of dynein activity. However, the above results indicate that neither the outer dynein arm, nor two of the three types of inner dynein arms, uniquely mediate the changes in flagellar motility required for phototaxis. The central pair complex and radial spokes are thought to function in flagellar regulation; defects in either of these structures causes flagellar paralysis (40, 41), and a group of second site suppressor mutations have been identified which restore function (14). Axonemes defective in radial spokes (*pf14*) or the central pair complex (*pf18*) both retained the 75-kD proteins. The 75-kD proteins were neither obviously enhanced nor missing in the mutant strain *uni1*, which lacks the *cis*-flagellum, suggesting that these proteins are not themselves differentially sorted between the two flagella. Thus, the location of the 75-kD proteins within the axoneme remains unknown.

The relationship between the two 75-kD proteins is not known. However, their migration in two-dimensional gels suggests that one may be a modified form of the other. Phosphorylation, resulting in the slightly more acidic form, is an obvious possibility, and may imply a means of regulation.

It should be noted that the specific calcium-binding protein or proteins within the axoneme which mediate phototaxis remain unknown. Calmodulin has been identified in the axoneme (8), and, like the 75-kD proteins, it does not appear to be a component of the dynein arms, radial spokes, or the central pair complex, and its precise location is unclear (28). It is thus possible that calmodulin and the 75-kD proteins are located together in a calcium-regulatory complex.

The authors thank Peter Nowell for generating the nonphototactic strain used in this work, Drs. Anthony Moss and Gregory Pazour for providing assistance with the phototaxis assay apparatus and analysis software, and Drs. Susan Dutcher, Elizabeth Harris, and Paul Lefebvre for providing advice and *Chlamydomonas* strains.

This work was supported by National Institutes of Health grants GM14228, GM30626, and CA12708.

Received for publication 25 August 1992 and in revised form 23 October 1992.

References

1. Batschelet, E. 1981. Circular Statistics in Biology. Academic Press Inc., London. 371 pp.
2. Bessen, M., R. B. Fay, and G. B. Witman. 1980. Calcium control of waveform in isolated flagellar axonemes of *Chlamydomonas*. *J. Cell Biol.* 86:446–455.
3. Dolle, R., J. Pfau, and W. Nultsch. 1987. Role of calcium ions in motility and phototaxis of *Chlamydomonas reinhardtii*. *J. Plant Physiol.* 126: 467–473.
4. Feinleib, M. E. 1985. Behavioral studies of free-swimming photoresponsive organisms. *In* Sensory Perception and Transduction in Aneural Organisms. G. Colombetti and P.-S. Song, editors. Plenum Publishing Corp., New York. 119–146.
5. Foster, K. W., and R. D. Smyth. 1980. Light antennas in phototactic algae. *Microbiol. Rev.* 44:572–630.
6. Foster, K. W., J. Saranak, N. Patel, G. Zarilli, M. Okabe, T. Kline, and K. Nakanishi. 1984. A rhodopsin is the functional photoreceptor for phototaxis in the unicellular eukaryote *Chlamydomonas*. *Nature (Lond.)*. 311:756–759.
7. Garrels, J. I. 1979. Two-dimensional gel electrophoresis and computer analysis of proteins synthesized by clonal cell lines. *J. Biol. Chem.* 254:7961–7977.
8. Gitelman, S. E., and G. B. Witman. 1980. Purification of calmodulin from *Chlamydomonas*: calmodulin occurs in cell bodies and flagella. *J. Cell Biol.* 87:764–770.
9. Harris, E. H. 1989. The *Chlamydomonas* Sourcebook: A Comprehensive Guide to Biology and Laboratory Use. Academic Press, Inc., San Diego, CA. 780 pp.
10. Hasegawa, E., H. Hayashi, S. Asakura, and R. Kamiya. 1987. Stimulation of in vitro motility of *Chlamydomonas* axonemes by inhibition of cAMP-dependent phosphorylation. *Cell Motil. Cytoskel.* 8:302–311.
11. Hegemann, P., W. Gartner, and R. Uhl. 1991. All-*trans* retinal constitutes the functional chromophore in *Chlamydomonas* rhodopsin. *Biophys. J.* 60:1477–1489.
12. Holmes, J. A., and S. K. Dutcher. 1989. Cellular asymmetry in *Chlamydomonas reinhardtii*. *J. Cell Sci.* 94:273–285.
13. Huang, B., Z. Ramanis, S. K. Dutcher, and D. J. L. Luck. 1982. Uniflagel-

lar mutants of *Chlamydomonas*: evidence for the role of basal bodies in transmission of positional information. *Cell.* 29:745–753.
14. Huang, B., Z. Ramanis, and D. J. L. Luck. 1982. Suppressor mutations in *Chlamydomonas* reveal a regulatory mechanism for flagellar function. *Cell.* 28:115–124.
15. Kamiya, R., and E. Hasegawa. 1987. Intrinsic difference in beat frequency between the two flagella of *Chlamydomonas reinhardtii*. *Exp. Cell Res.* 173:299–304.
16. Kamiya, R., and M. Okamoto. 1985. A mutant of *Chlamydomonas reinhardtii* that lacks the flagellar outer dynein arm but can swim. *J. Cell Sci.* 74:181–191.
17. Kamiya, R., and G. B. Witman. 1984. Submicromolar levels of calcium control the balance of beating between the two flagella in demembranated models of *Chlamydomonas*. *J. Cell Biol.* 98:97–107.
18. Kamiya, R., E. Kurimoto, and E. Muto. 1991. Two types of *Chlamydomonas* flagellar mutants missing different components of inner-arm dynein. *J. Cell Biol.* 112:441–447.
19. King, S. M., T. Otter, and G. B. Witman. 1986. Purification and characterization of *Chlamydomonas* flagellar dyneins. *Methods Enzymol.* 134: 291–306.
20. King, S. M., C. G. Wilkerson, and G. B. Witman. 1991. The Mr 78,000 intermediate chain of *Chlamydomonas* outer arm dynein interacts with alpha-tubulin *in situ*. *J. Biol. Chem.* 266:8401–8407.
21. Melkonian, M., and H. Robenek. 1980. Eyespot membranes of *Chlamydomonas reinhardtii*: a freeze-fracture study. *J. Ultrastruct. Res.* 72: 90–102.
22. Morel-Laurens, N. 1987. Calcium control of phototactic orientation in *Chlamydomonas reinhardtii:* Sign and strength of response. *Photochem. Photobiol.* 45:119–128.
23. Morel-Laurens, N. M. L., and M. E. Feinleib. 1983. Photomovement in an "eyeless" mutant of *Chlamydomonas*. *Photochem. Photobiol.* 37: 189–194.
24. Morrissey, J. H. 1981. Silver stain for proteins in polyacrylamide gels: a modified procedure with enhanced uniform sensitivity. *Anal. Biochem.* 117:307–310.
25. Nultsch, W. 1979. Effect of external factors on phototaxis of *Chlamydomonas reinhardtii*. III. Cations. *Arch. Microbiol.* 123:93–99.
26. Nultsch, W. 1983. The photocontrol of movement of *Chlamydomonas*. *Symp. Soc. Exp. Biol.* 36:521–539.
27. O'Farrell, P. H. 1975. High resolution two-dimensional electrophoresis of proteins. *J. Biol. Chem.* 250:4007–4021.
28. Otter, T. 1989. Calmodulin and the control of flagellar movement. Chapter 21. *In* Cell Movement. Volume 1. The Dynein ATPases. F. D. Warner, P. Satir, and I. R. Gibbons, editors. Alan R. Liss, Inc., New York. 281–298.
29. Pfister, K. K., R. B. Fay, and G. B. Witman. 1982. Purification and polypeptide composition of dynein ATPases from *Chlamydomonas* flagella. *Cell Motil.* 2:525–547.
30. Piperno, G., and D. J. L. Luck. 1979. Axonemal adenosine triphosphatases from flagella of *Chlamydomonas reinhardtii*. Purification of two dyneins. *J. Biol. Chem.* 254:3084–3090.
31. Piperno, G., B. Huang, Z. Ramanis, and D. J. L. Luck. 1981. Radial spokes of *Chlamydomonas* flagella: polypeptide composition and phosphorylation of stalk components. *J. Cell Biol.* 88:73–79.
32. Rüffer, U., and W. Nultsch. 1985. High-speed cinematographic analysis of the movement of *Chlamydomonas*. *Cell Motil.* 5:251–263.
33. Rüffer, U., and W. Nultsch. 1987. Comparison of the beating of cis- and trans-flagella of *Chlamydomonas* cells held on micropipettes. *Cell Motil. Cytoskeleton.* 7:87–93.
34. Rüffer, U., and W. Nultsch. 1990. Flagellar photoresponses of *Chlamydomonas* cells held on micropipettes: I. Change in flagellar beat frequency. *Cell Motil. Cytoskeleton.* 15:162–167.
35. Rüffer, U., and W. Nultsch. 1991. Flagellar photoresponses of *Chlamydomonas* cells held on micropipettes: II. Change in flagellar beat pattern. *Cell Motil. Cytoskeleton.* 18:269–278.
36. Sakakibara, H., and R. Kamiya. 1989. Functional recombination of outer dynein arms with outer arm-missing flagellar axonemes of a *Chlamydomonas* mutant. *J. Cell Sci.* 92:77–83.
37. Stavis, R. L. and R. Hirschberg. 1973. Phototaxis in *Chlamydomonas reinhardtii*. *J. Cell Biol.* 59:367–377.
38. Takahashi, T., K. Yoshihara, M. Watanabe, M. Kubota, R. Johnson, F. Derguini, and K. Nakanishi. 1991. Photoisomerization of retinal at 13-ene is important for phototaxis of *Chlamydomonas reinhardtii*: Simultaneous measurements of phototactic and photophobic responses. *Biochem. Biophys. Res. Comm.* 178:1273–1279.
39. Witman, G. B. 1986. Isolation of *Chlamydomonas* flagella and flagellar axonemes. *Methods Enzymol.* 134:280–290.
40. Witman, G. B., R. Fay, and J. Plummer. 1976. *Chlamydomonas* mutants: evidence for the roles of specific axonemal components in flagellar movement. *In* Cell Motility. R. D. Goldman, T. D. Pollard, and J. L. Rosenbaum, editors. Cold Spring Harbor Laboratory, Cold Spring Harbor, N.Y. 969–986.
41. Witman, G. B., J. Plummer, and G. Sander. 1978. *Chlamydomonas* flagellar mutants lacking radial spokes and central tubules. Structure, composition, and function of specific axonemal components. *J. Cell Biol.* 76:729–747.